Persistent currents and quantised vortices in a polariton superfluid

D. Sanvitto,[1,*] F. M. Marchetti,[2,†] M. H. Szymańska,[3] G. Tosi,[1]
M. Baudisch,[1] F. P. Laussy,[4] D. N. Krizhanovskii,[5] M. S. Skolnick,[5]
L. Marrucci,[6] A. Lemaître,[7] J. Bloch,[7] C. Tejedor,[2] and L. Viña[1]

[1]*Departamento de Física de Materiales, Universidad Autónoma de Madrid, Madrid 28049, Spain*

[2]*Departamento de Física Teórica de la Materia Condensada, Universidad Autónoma de Madrid, Madrid 28049, Spain*

[3]*Department of Physics, University of Warwick, Coventry, CV4 7AL, UK*

[4]*School of Physics and Astronomy, University of Southampton, Southampton, SO17 1BJ, UK*

[5]*Department of Physics and Astronomy, University of Sheffield, Sheffield, S3 7RH, UK*

[6]*Dipartimento di Scienze Fisiche, Università di Napoli Federico II and CNR-SPIN, Napoli, Italy*

[7]*LPN/CNRS, Route de Nozay, 91460, Marcoussis, France*

(Dated: January 18, 2011)

After the discovery of zero viscosity in liquid helium, other fundamental properties of the superfluidity phenomenon have been revealed. One of them, irrotational flow, gives rise to quantised vortices and persistent currents. Those are the landmarks of superfluidity in its modern understanding. Recently, a new variety of dissipationless fluid behaviour has been found in microcavities under optical parametric regime. Here we report the observation of metastable persistent polariton superflows sustaining a quantised angular momentum, m, after applying a 2 ps pulsed probe carrying a vortex state. We observe a transfer of angular momentum to the condensate steady state, which sustains vorticity for as long as it can be tracked. Furthermore, we study the stability of quantised vortices with $m = 2$. The experiments are analysed via a generalised two-component Gross-Pitaevskii equation. These results, aside from demonstrating the control of metastable persistent currents, show the peculiar superfluid character of non-equilibrium polariton condensates.

In the past few decades there has been a strenuous search for macroscopic coherence and phenomena related to Bose-Einstein condensation (BEC) in the solid state. The first realisation of a BEC in semiconductor microcavities [1] has inaugurated a new era in the study of strongly coupled light-matter systems. The growing interest in this field can be attributed to the unique properties of exciton-polaritons in microcavities [2], the composite particles resulting from strong light-matter coupling. The properties of a polariton condensate [3] differ from those of other known condensates, such as ultracold atomic BECs and superfluid ^{4}He. In particular, polaritons have a short lifetime of the order of picoseconds, therefore needing continuous pumping to balance decay and reach a steady state regime. Rather than a drawback, the intrinsic non-equilibrium nature enriches the features of polariton condensation, but at the same time poses fundamental questions about the robustness of the coherence phenomena to dissipation and non-equilibrium. Superfluid properties of non-equilibrium condensates in dissipative environment still need to be understood [4]. In this work, to advance in this direction, we investigate the hallmark of superfluidity, namely, vortices and metastable persistent flows.

Polariton superfluid phases out of equilibrium

One route to inject polaritons into a microcavity is by non-resonant (incoherent) pumping. For incoherent pumping, polaritons have been shown to enter, within their short lifetime, a macroscopically coherent BEC phase [1, 5, 6]. However, the unusual form of the excitation spectrum—diffusive at small momenta—hinders the fulfilling of the Landau criterion and puts under debate the possibility of dissipationless superflow in incoherently pumped polariton systems [7–9]. Because of the non-equilibrium nature of the polariton condensate in an inhomogeneous system, there are spontaneous supercurrents that may carry polaritons from gain to loss dominated regions. This can give rise to spontaneous formation of deterministic vortices, that do not necessarily imply superfluidity [4, 10]. Another peculiarity of polariton systems is to be found in their polarization, giving rise to a nomenclature of half-vortices [11, 12].

A different scenario characterises coherent resonant injection of parametrically pumped polariton condensates, which have been recently shown to exhibit a new form of non-equilibrium superfluid behaviour [13, 14]. In the optical parametric oscillator (OPO) regime [15], bosonic final state stimulation causes polariton pairs to coherently scatter from the pump state to the signal and idler states, which, at threshold, have a state occupancy of order one. The properties of the quantum fluids generated by OPO at idler and signal have been recently tested via a triggered optical parametric oscillator (TOPO) configuration [13]. An additional weak pulsed probe laser beam has been used to create a traveling, long-living, coherent polaritons signal, continuously fed by the OPO. The traveling signal has been shown to display superfluid behaviour through frictionless flow. However, long-lived quantised vortices and metastable persistent flow, i.e., another possible steady state of the condensate, still remained missing in the superfluid 'checklist' [4]. In this work, we fill-in this gap and we also address the case of higher winding numbers, unravelling a rich dynamics of vortices in polariton condensates. For this purpose, we use a technique already applied in non-linear and quantum optics, cold atoms and biophysics [16]: excitation by a light field carrying orbital angular momentum (OAM). Transfer of light OAM has been demonstrated in parametric processes in non-linear materials [17, 18] and has been used to generate atomic vortex states in Bose-Einstein condensates [19, 20].

Generation of persistent currents

In our experiment, the vortex is excited by a pulsed probe resonant with the signal (see Fig. 1) lasting only 2 ps. In other words, we stir the polariton superfluid only for a short time and observe its long lived rotation with a quantum of angular momentum on a time scale almost 70 times longer than the duration of the pulse (see Figs. 2 and 3). Although there is a similarity with rotating trapped gases, the effect for driven, non-equilibrium systems shows a richer phenomenology as will be described in the rest of this paper. Beside, a characteristic of vortices with higher winding number m is the tendency to coherently split into many vortices of $m = 1$ [21]. To study the stability properties of vortices in polariton condensates, we have injected a vortex with $m = 2$ and observed its evolution (see Fig. 4). Surprisingly, we found three different behaviours depending on the initial condition. In cases for which the vortex is imprinted into the signal steady state, one topological charge is always expelled out of the condensate (Fig. 4 (g-i)). On the other hand, when the vortex is not imprinted in the steady state but lasts only as long as the perturbation of the signal, we observe either a stable vortex of $m = 2$ when the probe carrying the vortex is at small momentum, resulting in a static (or slowly moving) vortex and slow supercurrents, or a splitting in two vortices of $m = 1$ when the vortex is injected with a probe at higher momentum. In the latter case, the vortex is moving faster than when it does not split, but still slower than the supercurrents of the condensate. Instability of doubly quantised vortices in a BEC has been observed in several systems [21], but there are only a few examples of their stability, such as in superconductors in the presence of pinning forces [22] or in a multicomponent order parameter superfluid such as ^{3}He-A [23]. In ultra-cold atomic gases, stable free $m = 2$ vortices have been theoretically predicted for some range of densities and interaction strengths [24]. However, they have been observed only in a toroidal pinning potential with an external optical plug [20], and demonstrated to split soon after the plug has been removed. The stability of $m = 2$ static vortex in polariton systems provides an additional experimental realization.

We use a semiconductor microcavity with a Rabi splitting $\Omega_R = 4.4$ meV and the cavity photon energy slightly negatively detuned (between 1 and 3 meV) from the exciton energy; see the Method section for details. A Ti-Sapphire laser is tuned in resonance with the lower polariton branch (LPB), injecting polaritons close to the point of inflection and giving rise to a continuously pumped OPO (see Fig. 1). Above a pump threshold, the signal generated

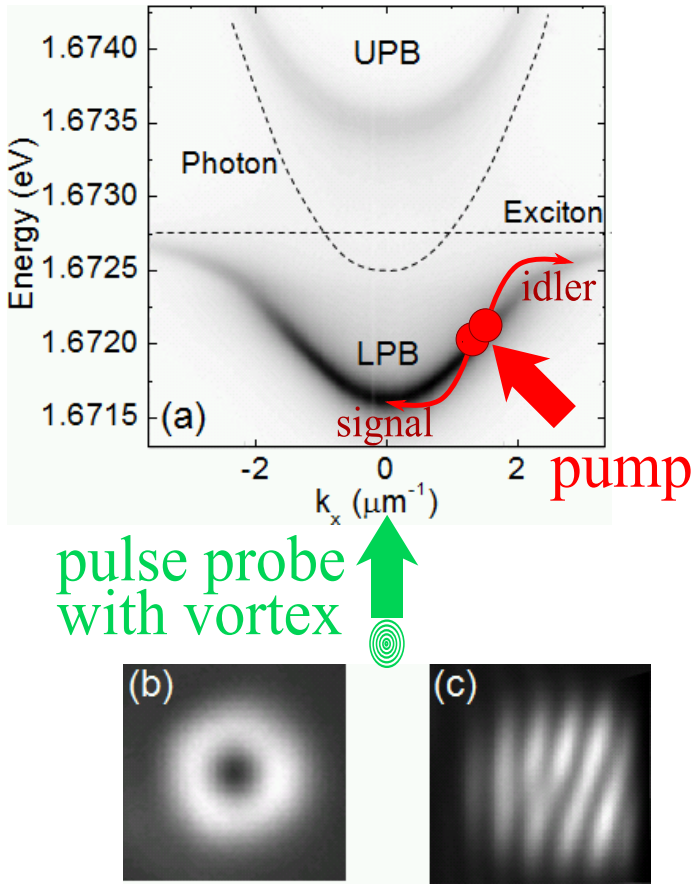

FIG. 1: Lower (LPB) and upper polariton branch (UPB) dispersions together with the schematic representation of the TOPO excitation (a). Resonantly pumping the LPB initiates, above threshold, stimulated scattering to a signal close to zero momentum and an idler at higher momentum. The $m = 1$ Laguerre-Gauss beam resonant with the signal (b) is used as a weak pulsed triggering probe to stir the superfluid. The corresponding interference image is shown in panel (c).

close to zero momentum ($\mathbf{k}_s = 0$) as well as the idler state at high momentum, form an out-of-equilibrium coherent polariton superfluid. At a given time, we trigger a new scattering process on top of the OPO signal with a resonant pulsed probe. The size of the probe is smaller than that of the signal (by a factor ≈ 4) to allow free motion of the vortex within the condensate, thus avoiding a spurious confinement. The probe is a pulsed Laguerre-Gauss beam carrying a vortex of given angular momentum m, the phase of which winds around the vortex core with values from 0 to $2\pi m$. After a short time, ~ 2 ps, the probe vanishes, leaving the polariton coherent state free to rotate, without the driving field. While even a classical fluid acquires angular momentum in the presence of an external rotating drive, only

a superfluid can exhibit infinitely lived circulating flow in a dissipative environment once the external drive is turned off. In order to demonstrate persistence of the vortex angular momentum, we detect the phase pattern generated by making interfere the polariton signal with an expanded and flipped spatial region far from the vortex core (where the phase is approximately constant) in a Michelson interferometer. A fork-like dislocation with a difference of m arms corresponds to phase winding by $2\pi m$ around the vortex core (see lower panel of Fig. 1).

Vortex dynamics

Using a streak camera we can follow the evolution in time of the vortex generated by the pulsed probe. Time intervals of 4 ps are used to reconstruct 2D images of the signal state after the perturbation has arrived. Every picture is the result of an average over many shots, all taken at the same time and same conditions. In order to separate the contribution of the signal from that of the pump, we filter, both in theory and experiments, the signal images in momentum space in a cone around $\mathbf{k} = 0$ of approximately $\pm 7^{\circ}$. At time t_{pb}, the pulsed laser probe is shined on the sample. Its general effect is to enhance the polariton signal emission by a factor that ranges, depending on the experiment, between a few percent to more than 100 % with a delay of 10 ps after the pulse arrival time. At first a strong gain given by the presence of the probe creates an extra population on top of the OPO signal (called TOPO polaritons) before the OPO signal is re-established. We follow the evolution of the transient state and monitor how the probe affects the condensate in its steady state. We find that the original steady state can be recovered but also, more interestingly, that different stable solutions are possible.

The time evolution of an excited $m = 1$ vortex together with its interference pattern, which characterises unequivocally the vortex state, are shown in Fig. 2, where the external probe has a power of 6.6 μW, which is less than the OPO signal emission before the probe arrives on the sample. In these images, we can observe two effects: immediately after the arrival of the probe, a vortex is generated in the TOPO polaritons and its vorticity is maintained although the population decays in a few tenths of picoseconds. After the extra polaritons have disappeared, the vortex remains imprinted into the steady population of the condensate. While the polariton vorticity is always present and enduring in the TOPO

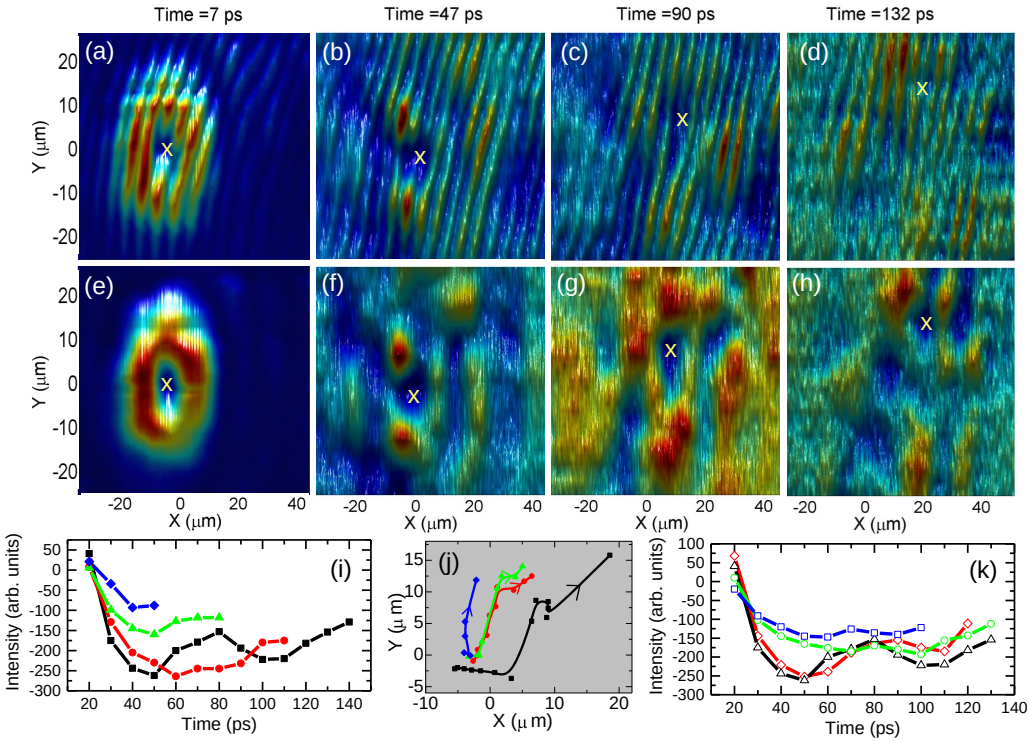

FIG. 2: Time evolution of the polariton signal after a weak pulsed probe with a vortex of $m = 1$ has been excited (a-h). The interference images (a-d) are obtained by overlapping the vortex with a small expanded region of the same image far from the vortex core, where the phase is constant. The time origin is taken when the extra population has reached 80% of its maximum value. To better reveal the effect of the imprinting of the vortex into the condensate steady state of the signal, the contribution of the unperturbed polariton signal (in absence of the probe pulse) is subtracted from all data. The depth of the vortex core and its position as a function of time for 4 different pump powers (65 mW, blue diamonds, 100 mW, green triangles, 200 mW red circles, 300 mW, black squares)—all above the OPO threshold (50 mW)—is shown in (i) and (j) respectively. The effect of probe power—0.15 μW in blue squares, 0.33 μW in green circles, 6.65 μW in black triangles, 8 μW in red diamonds—on the duration and depth of the core of the vortex is shown in (k).

polaritons, only under very high pump power and at specific points in the sample is the vorticity also passed to the steady state of the OPO signal. This not only demonstrates that polariton condensates show unperturbed rotation, but also that a vortex is another stable solution of the final steady state. This is a clear demonstration of superfluid behaviour in the non-equilibrium polariton OPO system. These effects are visible in the real space images through the 'toroidal shape' of the polariton emission at early times, and the presence of a fork dislocation in the interference images at all times. The latter show that the spatial phase relation remains constant and with full contrast all over a wide area, even for times much longer than the signal coherence time, as measured by detecting the decay of interference-fringe contrast when delaying the signal and the reference (see Fig. 6 in the supplementary material). This means that even when polaritons have lost any phase relation in time, their angular momentum is still conserved.

After the vortex is imprinted into the OPO signal, we can observe the vortex core slowly drifting to the right and then upwards changing in shape and moving with different velocities. The drift is due to the fact that the vortex core is naturally inclined to undergo a random walk and eventually either remains permanently trapped in the condensate or is expelled from the edges (see the following theory and Ref. [25]). However, due to the presence of local defects [26], which tend to influence the motion of the vortex, the path followed by the vortex core recurs at each repetition of the experiment. For this reason we are able to track its movement that otherwise would be washed out by the experimental averaging.

Figures 2 (i,j) and (k) show the effect of pump and probe powers on the transfer of angular momentum to the condensate steady state. Note that to highlight this effect, all the data shown in this paper have been obtained by subtracting the steady state of the condensate unperturbed by the probe pulse. As a consequence, the depth of the vortex core comes out with negative values. An increase of the power of the pump helps the observation of this effect possibly due to an enhancement of the OPO coherence for higher pumping intensities. Above four times the OPO threshold, we observe a saturation in the depth of the core [see intensity at 50 ps in Fig. 2 (i)]. However given the different pathways followed by the vortex when changing pump intensity [see Fig. 2 (j)], a variation of the depth in time is also expected, depending on the kind of inhomogeneities met by the vortex along its trajectory. As for the probe, we find that a minimum power is required for the polaritons to acquire enough angular momentum to be able to transfer it to the steady state. This rigidity of the

fluid to accommodate a vortex at low intensities has also been predicted for incoherently pumped polariton condensates [25]. However, once the transfer is achieved, the probe power does not change significantly the duration and depth of the vortex in the steady state. An alternative interpretation of the short vortex lifetime, for low excitation powers, could be attributed to dissipation when the average angular velocity is higher than some critical velocity–leading to the onset of macroscopic drag forces (like recently discussed for non-resonant pumping in Ref. [9]). Therefore, taking the difference between opposite momenta across the vortex core, we have obtained the average angular velocity to be ~ 0.2 μm/ps. This value sets a lower bound for the critical velocity, which depends on polariton densities and, for small pumping powers, could be the cause of short lasting times for the polariton vorticity.

The sequence in Fig. 2 demonstrates that the vortex remains steady as a persisting metastable state for times much longer than the extra population created by the probe pulse and eventually gets imprinted in the steady state of the OPO signal. This is revealed by the strong contrast of the fork in the interference images for as long as the core remains within the condensate area. In the opposite scenario—dissipation of angular momentum as for classical fluids—the interference images would show low contrast in the vortex core region, indicating a mixture of the population which has undergone dissipation and the one still carrying the quantised angular momentum.

In our experiments we have measured an average size of the core radius between 4 and 5 μm. This is in good agreement with a theoretical estimate of the healing length $\xi \simeq \pi/\sqrt{2m_{LP}\delta E}$, where m_{LP} is the lower polariton mass and δE is the lower polariton blue-shift, determined by the polariton-polariton interaction strength.

Numerical simulations

We have numerically simulated the experiments by making use of mean-field two-component Gross-Pitaevskii equations for the coupled cavity and exciton fields with external pump and decay; see the Method section for details. We have chosen parameters close to the experimental ones, finding first the conditions for OPO. In the simulation of Fig. 3, we consider a pump with strength $f_p = 1.24 f_p^{(\mathrm{th})}$ above OPO threshold, and once the steady state is reached (left panel), we turn on the probe carrying a vortex $m = 1$, resonant with the

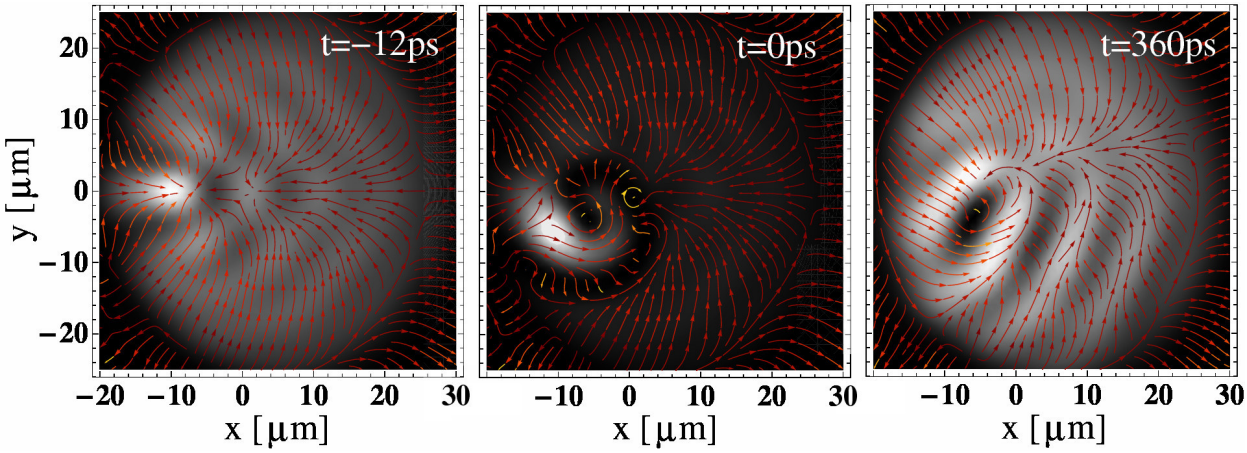

FIG. 3: Numerical simulations of the time evolution of the OPO signal before and after the arrival ($t = 0$) of a pulsed probe carrying an $m = 1$ vortex resonant with the signal momentum and energy, for pumping strength $f_p = 1.24 f_p^{(\mathrm{th})}$ above OPO threshold. The images of the signal are obtained by momentum filtering in a cone of around $\pm 7°$. The pulse carrying the vortex generates a gain which fades out after about 10 ps leaving an $m = 1$ vortex imprinted into the signal. The vortex experiences a transient time of around 30 ps before settling into a metastable solution. The supercurrents are plotted in the frame of the signal by subtracting the $\mathbf{k}$ of the signal.

signal for 2 ps only. We observe a gain of the signal (central panel) for around 10 ps which is followed by a transient time during which the imprinted vortex drifts around inside the signal. For the simulation shown in Fig. 3, the transient lasts for about 30 ps, after which the vortex settles into a metastable solution lasting around 400 ps. In addition, we also find stable steady-state (i.e., infinitely lived) vortex solutions, analogous to the ones reported in Ref. [27]. Such a solution does not always exist and it strongly depends on the pumping conditions: in other cases, during the transient period, the excited vortex either spirals out of the signal or recombines with an antivortex forming at the edge of the signal. There are also cases where, instead, the imprinted vortex settles into a metastable state, which can last several hundred picoseconds as shown in Fig. 3, and then starts drifting again. We have also analysed the dependence of the vortex solutions on the probe intensity and found that for steady-state vortex solutions there is no dependence on the probe intensity, which can only affect the duration of the transient period. However, for metastable solutions, we found a threshold in the probe power, below which the vortex does not get imprinted into the

signal anymore. Thus the results of the theoretical simulations are in excellent qualitative agreement with the experimental observations.

Doubly quantised vortices

A second experiment is aimed at investigating the stability of doubly quantised vortices in different regimes. We perform both experiments and numerical simulations in conditions similar to the ones previously described, but now considering a pulsed probe carrying a doubly quantised vortex $m = 2$. We demonstrate three distinctive behaviours (see Fig. 4) by repeating the experiments under different conditions. For cases in which the vortex lasts as long as the TOPO population is present, we observe that when the vortex is excited on a static signal centered at $\mathbf{k} = 0$, it does not split within its lifetime [Fig. 4 (a-c)]. However, exciting the signal with a finite momentum, thus making it moving inside the pump spot, we observe the doubly quantised vortex splitting into two singly quantised vortices, as shown in Fig. 4 (d-f).

Our theoretical analysis gives the same result: a TOPO vortex (below the OPO threshold) is stable when it is either at rest or moves below a critical velocity, and splits otherwise (see Fig. 5). In order to explain this result, we have analysed the supercurrents characterizing the signal. We found that, below threshold, these supercurrents are a superposition of the vortex currents with a net current corresponding exactly to the momentum $\mathbf{k}_{pb}$ at which the probe has been injected. In addition, we have evaluated the group velocity $\mathbf{v}_g$ at which the triggered signal (carrying the vortex) moves in real space. We found that $\mathbf{v}_g$ increases linearly with $\mathbf{k}_{pb}$ up to a critical value, $\mathbf{k}_{pb}^{cr}$, and sublinearly above. Therefore, we expect that in the frame of the moving vortex, there is no net current in the linear regime, while, in the sublinear regime, the vortex feels a net current which causes it to split (see Fig. 5). Indeed, we observe that the $m = 2$ vortex splits exactly when is injected at or above $\mathbf{k}_{pb}^{cr}$. Note that a TOPO signal is a decaying state, therefore the $m = 2$ vortex can be stable only within its lifetime.

In the case when, instead, the vortex is also imprinted into the OPO steady-state, we observe that the $m = 2$ vortex splits, one $m = 1$ vortex is quickly expelled outside the signal, while the other vortex stabilizes and persists, as is also the case in the experiment, see Fig. 4 (g-i). Numerical simulations show that above OPO threshold the structure of the currents

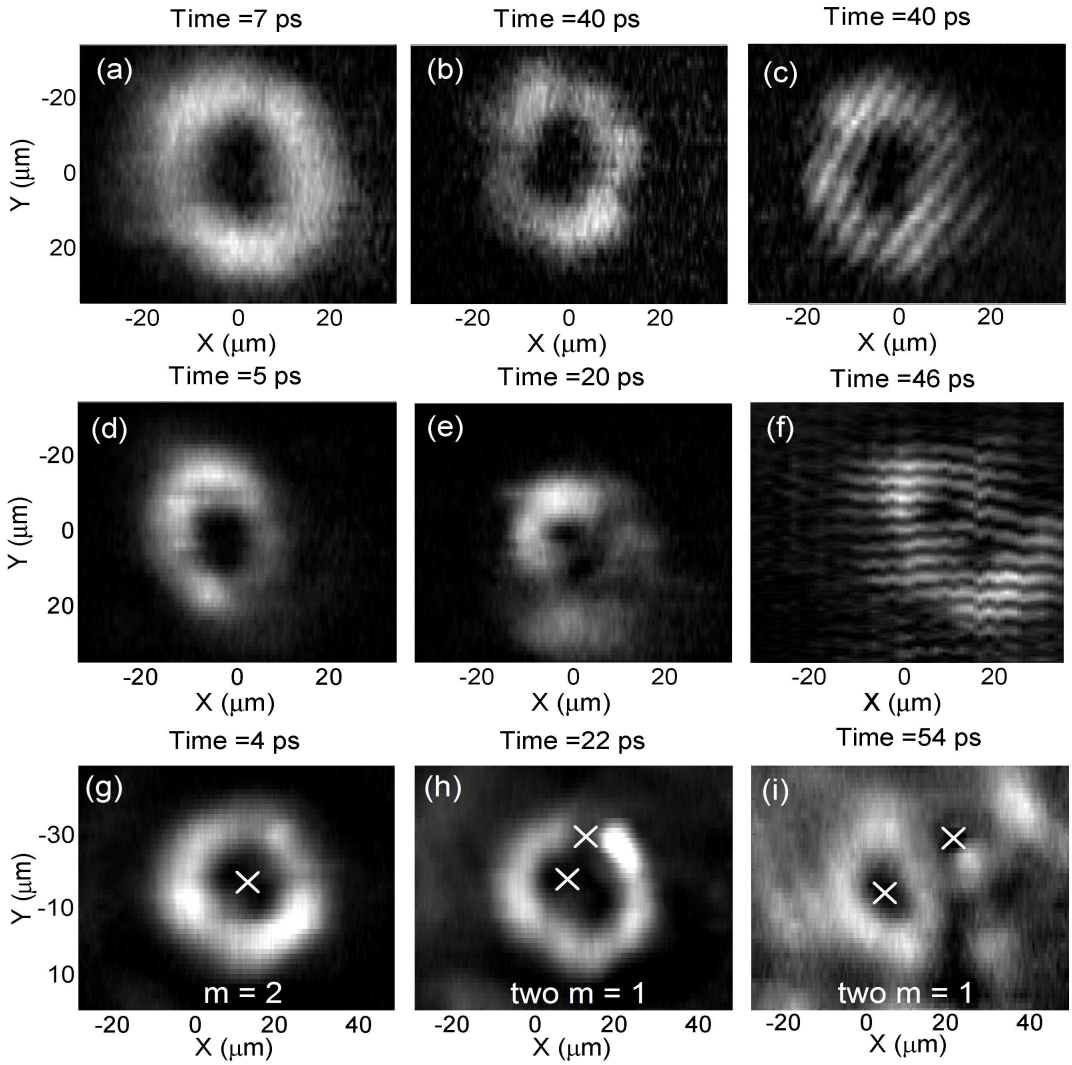

FIG. 4: Time evolution of a $m = 2$ vortex TOPO signal excited close to zero momentum, $\mathbf{k} = 0$, (a-c) for which neither motion nor splitting of the vortex could be detected. However for a signal at $\mathbf{k}_s$ pointing to the right (d-f), we can detect the $m = 2$ vortex both moving and splitting into two single quantised $m = 1$ vortices. In the last panel of the first two rows we plot the interference images corresponding to a late time. In both experiments the vortex is only present in the TOPO population. On the contrary, when the vortex is imprinted into the OPO state, then the situation is as shown in the images (g-i). Here the splitting appears immediately after the angular momentum is transfered to the steady state (≈ 20 ps) and only one of the two vortices of $m = 1$ survives, the other being expelled from the condensate in the first 40 ps.

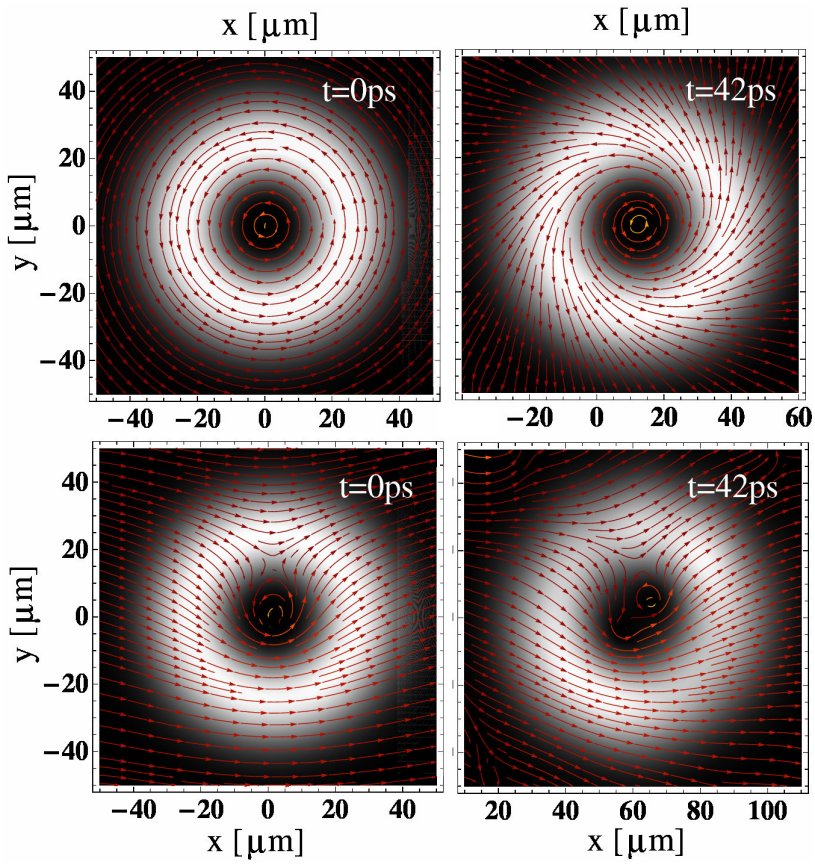

FIG. 5: Calculated TOPO signal emission for a $m = 2$ triggering probe at $\mathbf{k}_{pb} = 0.1\ \mu\text{m}^{-1} < \mathbf{k}_{pb}^{cr}$ (first row) and at $\mathbf{k}_{pb} = 0.7\ \mu\text{m}^{-1} > \mathbf{k}_{pb}^{cr}$ (second row) at the arrival of the probe ($t = 0$) and 42 ps after. The supercurrents are plotted in the frame of the group velocity of the moving vortex. In the second row, the net current felt by the $m = 2$ vortex causes it to split.

in the signal is complex and thus a stationary vortex will always feel a net current. This is the reason why above OPO we always observe splitting of the $m = 2$ vortex.

Acknowledgements

We are grateful to D. Whittaker, J. J. García-Ripoll, P. B. Littlewood and J. Keeling for stimulating discussions. This work was partially supported by the Spanish MEC (MAT2008-01555 and QOIT-CSD2006-00019) and the CAM (S2009/ESP-1503). DS and FMM acknowledge financial support from the Ramón y Cajal program. GT thanks the FPI scholarship from the Ministry of Education. We would like to thank TCM group (Cavendish Laboratory,

Cambridge, UK) for the use of computer resources. Requests should be addressed to D.S. for experimental details and to F.M.M. for theoretical matters.

Author contributions

D.S., G.T. and M.B. carried out the experiments. F.M.M. and M.H.S. performed the theoretical simulations. L.M. provided the holograms for getting vortex excitation and A.L. and J.B. fabricated the samples. All the authors analysed the results, discussed the underlying physics and contributed to the manuscript.

METHODS

Experiments

The sample studied is a $\lambda/2$ AlAs microcavity with a 20 nm GaAs quantum well placed at the antinode of the cavity electromagnetic field. The cavity is formed by two high reflective Bragg mirrors of 25 pairs at the bottom and 15.5 on the top of the structure. The pump is obtained with a cw Ti-Sapphire laser, resonantly exciting the LPB close to the inflection point at 9°. The spot size is of ≈ 100 μm.

The experiments are performed at a cryogenic temperature of 10 K and using a very high numerical aperture lens (0.6) so that the sample could be accessed by angles as large as 25° and the photoluminescence (PL) can be simultaneously collected from the signal state in the near as well as the far field. The PL was collected through a 0.5 m spectrometer into a streak camera, working in synchroscan mode, with 4 ps time resolution, allowing for energy—as well as time-resolved—images. In order to reach high time resolution, all the images where obtained by filtering the signal in the far field without spectrally resolving the emission of the OPO states. Differently from our TOPO experiment [28], here we excite and trigger with the probe at the signal state in a pumping regime above threshold.

The vortex probe state is prepared by scattering a Ti:Sapphire pulsed laser Gaussian beam in an hologram with a single or double fork-like dislocation. This gives rise to a first order Laguerre-Gauss beam with a winding number either $m = 1$ or $m = 2$, respectively. The probe beam is focused at the center of the cw pump in resonance with the signal emission energy and at around $\mathbf{k} = 0$ for most of the cases, except when a finite velocity is given to

the vortex state. In this latter case the probe is arriving on the sample with a finite angle, between one or two degrees, so that the vortex can have a finite velocity showing splitting of the $m = 2$ state. The probe is focussed in a region of ≈ 25 μm having a power set to be below the intensity of the signal. Moreover, considering the wide energy spread given by its fast duration (2 ps) the amount of power getting into the cavity is estimated to be between 1/10 and 1/5 of the signal emission. Every picture is the result of an average over many shots, as single shot measurements would give a too low signal to noise ratio.

A realization of optically transferring orbital angular momentum to atomic BECs, using Laguerre-Gauss beams, as in our experiments, was performed using a two-photon stimulated Raman process [19]. $m = 2$ were generated in a BEC of sodium atoms but its stability was not analysed.

Theory

The dynamics of amplitudes and phases of TOPO is analysed using two-component Gross-Pitaevskii equation with external pumping and decay for the coupled cavity and exciton fields $\psi_{C,X}(\mathbf{r}, t)$ ($\hbar = 1$):

$$i\partial_t \begin{pmatrix} \psi_X \\ \psi_C \end{pmatrix} = \begin{pmatrix} \omega_X - i\kappa_X + g_X|\psi_X|^2 & \Omega_R/2 \\ \Omega_R/2 & \omega_C - i\kappa_C \end{pmatrix} \begin{pmatrix} \psi_X \\ \psi_C \end{pmatrix} + \begin{pmatrix} 0 \\ F_p + F_{pb} \end{pmatrix} . \qquad (1)$$

Since the exciton mass is four orders of magnitude larger than the photon mass, we neglect the excitonic dispersion and assume a quadratic dispersion for the cavity photon, $\omega_C = \omega_C(0) - \nabla^2/2m_C$. The fields decay with rates $\kappa_{C,X}$. Ω_R is the photon-exciton coupling. The cavity field is driven by an external cw pump field,

$$F_p(\mathbf{r}, t) = f_p e^{-\frac{|\mathbf{r}-\mathbf{r}_p|^2}{2\sigma_p^2}} e^{i(\mathbf{k}_p \cdot \mathbf{r} - \omega_p t)} ,$$

while the probe is a Laguerre-Gaussian pulsed beam,

$$F_{pb}(\mathbf{r}, t) \simeq f_{pb}|\mathbf{r} - \mathbf{r}_{pb}|^m e^{-\frac{|\mathbf{r}-\mathbf{r}_{pb}|^2}{2\sigma_{pb}^2}} e^{im\varphi(\mathbf{r})} e^{-\frac{(t-t_{pb})^2}{2\sigma_t^2}} e^{i(\mathbf{k}_{pb} \cdot \mathbf{r} - \omega_{pb} t)} , \qquad (2)$$

producing a vortex at $\mathbf{r}_{pb}$ with winding number m. The exciton repulsive interaction strength g_X can be set to one by rescaling fields and pump strengths. We solve Eq. (1) numerically by using the 5^{th}-order adaptive-step Runge-Kutta algorithm on a 2D grid.

We take $m_C = 2.3 \times 10^{-5} m_0$ and a Rabi splitting $\Omega_R = 4.4\,\mathrm{meV}$ determined experimentally. In the regime of our experiments, we can neglect the saturation of the dipole coupling [29]. We choose the pumping angle $\mathbf{k}_p$, the energy of the pump ω_p and the pump profile as the experimental ones.

The calculated images of the signal in Figs. 3 and 5 are obtained by filtering in momentum space around the signal momentum, $\mathbf{k}_s$. We set to zero all the emission in momentum space aside the one coming from the signal and fast Fourier transform back to real space. In this way the strong emission coming at the pump angles is masked out.

SUPPLEMENTARY MATERIAL

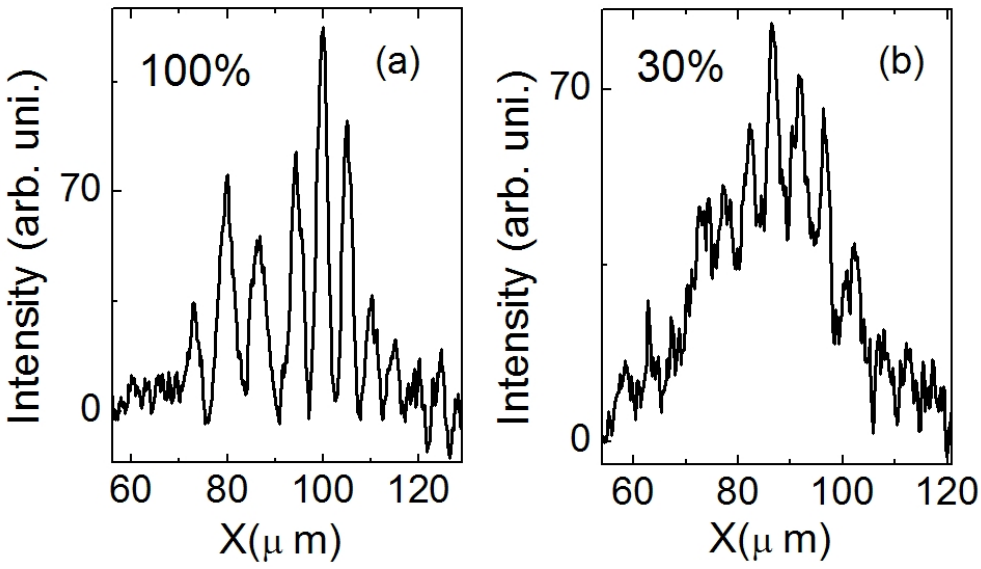

FIG. 6: Intensity of interference fringes (arbitrary units) of the polariton emission after arrival of the probe pulse. The two images are taken at different delay times between the polariton signal and its mirrored counterpart: (a) 0 ps and (b) 55 ps time delay.

In Fig. 6 we show the intensity of the interference fringes of the vortex with $m = 1$ (Fig. 2 of the main text) obtained with the Michelson interferometer but at different time delays between the two arms. Immediately after the probe has arrived, and at zero delay, the fringes exhibits a visibility close to 100%, while it reduces to 30% for a delay of 55 ps. However the interferences of the vortex core of Fig. 2—taken always at zero delay time—do not show any degradation of the visibility even for more than 100 ps after the probe has arrived, demonstrating the persistence of the polariton vorticity.

In Fig. 7 and 8 we show the calculated time evolution of a doubly quantised vortex in the case when it imprints into the OPO signal. In this regime, we see the vortex to split into two singly quantised vortices almost immediately when the probe arrives, already during the imprinting process. The two vortices coexist for a short time, after which one is expelled from the condensate, usually annihilating with an anti-vortex present at the signal boundary.

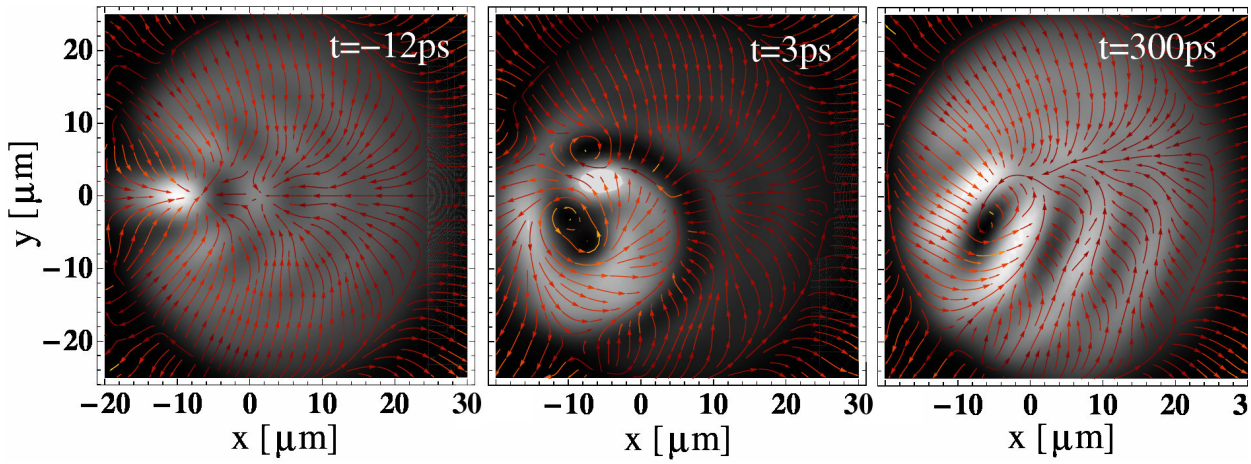

FIG. 7: Calculated time evolution of the OPO signal emission for a $m = 2$ triggering probe before the arrival of the probe at $t = 0$ and after, showing the splitting of the imprinted doubly quantised vortex, the expulsion from the signal of one $m = 1$ vortex and the stabilisation of the other $m = 1$ vortex into the signal. The supercurrents are plotted in the frame of the signal like in the Fig. 3.

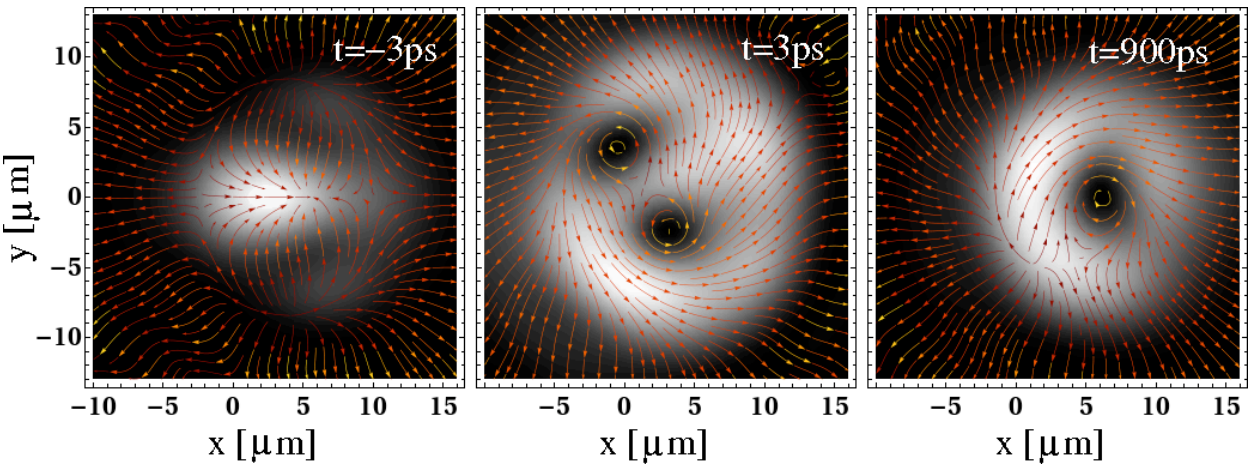

FIG. 8: Calculated time evolution of the OPO signal emission for a $m = 2$ triggering probe as in Fig. 7 but for smaller spatial size of the signal showing that the qualitative behaviour of doubly quantised vortices remains the same for smaller signals.

* Electronic address: daniele.sanvitto@uam.es

† Electronic address: francesca.marchetti@uam.es

[1] Kasprzak, J. *et al.* Bose-Einstein condensation of exciton polaritons. *Nature* **443**, 409–414 (2006).

[2] Weisbuch, C., Nishioka, M., Ishikawa, A. & Arakawa, Y. Observation of the coupled exciton-photon mode splitting in a semiconductor quantum microcavity. *Phys. Rev. Lett.* **69**, 3314–3317 (1992).

[3] Keeling, J., Marchetti, F. M., Szymańska, M. H. & Littlewood, P. B. Collective coherence in planar semiconductor microcavities. *Semicond. Sci. Technol.* **22**, R1–R26 (2006).

[4] Keeling, J. & Berloff, N. G. Going with the flow. *Nature* **457**, 273–274 (2009).

[5] Balili, R., Hartwell, V., Snoke, D., Pfeiffer, L. & West, K. Bose-Einstein condensation of microcavity polaritons in a trap. *Science* **316**, 1007–1010 (2007).

[6] Lai, C. W. *et al.* Coherent zero-state and π-state in an exciton-polariton condensate array. *Nature* **450**, 529–532 (2007).

[7] Szymańska, M. H., Keeling, J. & Littlewood, P. B. Nonquilibrium quantum condensation in an incoherently pumped dissipative system. *Phys. Rev. Lett.* **96**, 230602 (2006).

[8] Wouters, M. & Carusotto, I. Excitations in a nonequilibrium Bose-Einstein condensate of exciton polaritons. *Phys. Rev. Lett.* **99**, 140402 (2007).

[9] Wouters, M. & Carusotto, I. Are non-equilibrium Bose-Einstein condensates superfluid? (2010). Cond-mat/1001.0660.

[10] Lagoudakis, K. G. *et al.* Quantised vortices in an exciton-polariton fluid. *Nature Physics* **4**, 706–710 (2008).

[11] Rubo, Y. G. Half vortices in exciton polariton condensates. *Phys. Rev. Lett.* **99**, 106401 (2007).

[12] Lagoudakis, K. G. *et al.* Observation of half-quantum vortices in an exciton-polariton condensate. *Science* **326**, 974–976 (2009).

[13] Amo, A. *et al.* Collective fluid dynamics of a polariton condensate in a semiconductor microcavity. *Nature* **457**, 291–295 (2009).

[14] Amo, A. *et al.* Superfluidity of polaritons in semiconductor microcavities. *Nat. Phys.* **5**, 805–810 (2009).

[15] Stevenson, R. M. *et al.* Continuous wave observation of massive polariton redistribution by stimulated scattering in semiconductor microcavities. *Phys. Rev. Lett.* **85**, 3680–3683 (2000).

[16] Molina-Terriza, G., Torres, J. P. & Torner, L. Twisted photons. *Nat. Phys.* **3**, 305–310 (2007).

[17] Dholakia, K., Simpson, N. B., Padgett, M. J. & Allen, L. Secind harmonic generation and the orbital angular momentum of light. *Phys. Rev. A* **54**, R3742–R3745 (1996).

[18] Martinelli, M., Huguenin, J. A. O., Nussenzveig, P. & Khuory, A. Z. Orbital angular momentum exchange in an optical parametric oscillator. *Phys. Rev. B* **70**, 013812 (2004).

[19] Andersen, M. F. *et al.* Quantized rotation of atoms from photons with orbital angular momentum. *Phys. Rev. Lett.* **97**, 170406 (2006).

[20] Ryu, C. *et al.* Observation of persistent flow of a Bose-Einstein condensate in a toroidal trap. *Phys. Rev. Lett.* **99**, 260401 (2007).

[21] Shin, Y. *et al.* Dynamical instability of a doubly quantized vortex in a Bose-Einstein condensate. *Phys. Rev. Lett.* **93**, 160406 (2004).

[22] Baert, M., Metlushko, V. V., Jonckheere, R., Moshchalkov, V. V. & Bruynseraede, Y. Composite flux-line lattices stabilized in superconducting films by a regular array of artificial defects. *Phys. Rev. Lett.* **74**, 3269–3272 (1995).

[23] Blaauwgeers, R. *et al.* Double-quantum vortex in superfluid 3He-A. *Nature* **404**, 471–473 (2000).

[24] Möttönen, M., Mizushima, T., Isoshima, T., Salomaa, M. M. & Machida, K. Splitting of a doubly quantized vortex through intertwining in Bose-Einstein condensates. *Phys. Rev. A* **68**, 023611 (2003).

[25] Wouters, M. & Savona, V. Creation and detection of vortices in polariton condensates (2009). Cond-mat/0904.2966.

[26] Sanvitto, D. *et al.* Spatial structure and stability of the macroscopically occupied polariton state in the microcavity optical parametric oscillator. *Phys. Rev. B* **73**, 241308 (2006).

[27] Whittaker, D. Vortices in the microcavity optical parametric oscillator. *Superlatt. and Microstruct.* **41**, 297–300 (2007).

[28] Ballarini, D. *et al.* Observation of long-lived polariton states in semiconductor microcavities across the parametric threshold. *Phys. Rev. Lett.* **102**, 056402 (2009).

[29] Ciuti, C., P.Schwendimann & Quattropani, A. Theory of polariton parametric interactions in semiconductor microcavities. *Semicond. Sci. Technol.* **18**, S279–S293 (2003).